Ultrastructure of rhoptry development in *Plasmodium falciparum* erythrocytic schizonts

L. H. BANNISTER[1]*, J. M. HOPKINS[1,2], R. E. FOWLER[1,2], S. KRISHNA[3] *and* G. H. MITCHELL[2]

[1] *Department of Anatomy, Cell and Human Biology, GKT, Guy's Hospital, London SE1 1UL, UK*
[2] *Department of Immunobiology, GKT, Guy's Hospital, London SE1 9RT, UK*
[3] *Department of Infectious Diseases, St George's Hospital Medical School, Cranmer Terrace, London SW17 0RE, UK*

(*Received 12 January 2000; revised 9 March 2000; accepted 12 March 2000*)

SUMMARY

Prior to the separation of merozoites from the *Plasmodium falciparum* schizont, various stage-specific organelles are synthesized and assembled within each merozoite bud. The apical ends of the merozoites are initiated close to the ends of endomitotic spindles. At each of these sites, the nuclear membrane forms coated vesicles, and a single discoidal or cup-like Golgi cisterna appears. Reconstruction from serial sections indicates that this structure receives vesicles from the nuclear envelope and in turn gives off coated vesicles to generate the apical secretory organelles. Rhoptries first form as spheroidal structures and grow by progressive fusion of small vesicles around their margins. As each rhoptry develops, 2 distinctive regions separate within it, an apical reticular zone with electron-lucent areas separated by cords of granular material, and a more homogenously granular basal region. The apical part elongates into the duct, with evidence for further vesicular fusion at the duct apex. The rounded rhoptry base becomes progressively more densely packed to form a spheroidal mass, and compaction also occurs in the duct. Typically, one rhoptry matures before the other. Cryofractured rhoptry membranes show asymmetry in the sizes and numbers of intramembranous particles at the internally- and externally-directed fracture faces.

Key words: *Plasmodium falciparum*, schizont, rhoptry, Golgi complex, ultrastructure.

INTRODUCTION

Within the bloodstream of their vertebrate hosts, malaria parasites undergo repeated cycles of intracellular invasion, growth and multiplication. In *Plasmodium falciparum* the multiplicative stage (schizont) undergoes 4 rounds of endomitotic nuclear division before budding off about 16 merozoites from its perimeter, each able to invade another erythrocyte (Read *et al*. 1993; see also Vickerman & Cox, 1967 for *Plasmodium vinckei*). The mechanisms of coordinated synthesis, trafficking and emplacement of organelles within the maturing merozoite have yet to be determined (see the discussion by Shaw & Tilney, 1992, for the related genus *Theileria*), but are clearly of interest because of their relevance to antimalarial drug and vaccine development. The present paper is concerned with the formation of the merozoite rhoptries, pear-shaped secretory organelles which discharge their contents on to the red cell membrane during invasion to enclose the parasite in a membrane-lined (parasitophorous) vacuole (for reviews see Bannister & Dluzewski, 1990; Ward, Chitnis & Miller, 1994).

* Corresponding author: Department of Anatomy and Cell Biology, Centre for Neuroscience, Hodgkin Building, GKT, Guy's Hospital, London SE1 1UL, UK. Tel: +44 207 955 5000 X 5503. Fax: +44 207 848 6569. E-mail: lawrence.bannister@kcl.ac.uk

Rhoptries contain a considerable number of proteins (see Etzion, Murray & Perkins, 1991; Perkins, 1992), several of which have been localized by immunoelectron microscopy in either the rounded base (e.g. the proteins RAP1 and RAP2: Crewther *et al*. 1990) or the apical duct (including AMA-1, Crewther *et al*. (1990), a 225 kDa protein, Roger *et al*. (1988) and a 140/130/110 kDa family, Sam-Yellowe *et al*. (1995)). It has been shown in *P. falciparum* that rhoptry proteins RhopH-3, RAP1 and RAP2 are synthesized in the cytoplasm, and accumulate peripherally in small vesicles which grow into rhoptries (Jaikaria *et al*. 1993). In both *P. yoelii* (Ogun & Holder, 1994) and *P. falciparum* (Howard & Schmidt, 1995; Howard *et al*. 1998), rhoptry proteins translated in the endoplasmic reticulum require a brefeldin A-sensitive step for their maturation, indicating a route via a Golgi body. Ultrastructural evidence suggests that the secretory pathway in *Plasmodium* involves a minimal Golgi complex (Langreth *et al*. 1978; see also Tilney & Tilney, 1996; Ward, Tilney & Langsley, 1997) formed by fusion of vesicles derived from the nuclear envelope, as also in *Toxoplasma* (Vivier & Petitprez, 1972; Hager *et al*. 1999), although these structures have not been reported in detail in *Plasmodium*.

In the present paper we describe the structural development of rhoptries in the budding merozoite in relation to possible routes of protein targeting, as

https://doi.org/10.1017/S0031182099006320 Published online by Cambridge University Press

a basis for further experimental work (at present in progress). Some of these findings have been alluded to in a short review of the merozoite cytoskeleton (Bannister & Mitchell, 1995).

MATERIALS AND METHODS

Electron microscopy

P. falciparum of the ITO4, Paolo Alto and C10 strains were cultured and synchronized by standard methods (Lambros & Vanderberg, 1979). Schizont-infected red cells were concentrated on a Percoll cushion (Dluzewski *et al*. 1984), from parasitaemias between about 15 and 25%, as detailed elsewhere (Webb *et al*. 1996). After a brief wash in culture medium to remove adherent Percoll, these cells were allowed to grow for a further 30 min–1 h at 37 °C, and were then processed as detailed by Bannister & Mitchell (1989) for transmission electron microscopy (TEM). Briefly, fixation was carried out at room temperature for 3 h in 2·5% (v/v) glutaraldehyde and 0·75% (w/v) tannic acid, buffered at pH 7·0 with 0·1 M sodium cacodylate. Cells were washed 3 times by centrifugation in cacodylate buffer, pelletted, then post-fixed in 1% osmium tetroxide in cacodylate buffer, rinsed in distilled water and block stained with 1% aqueous uranyl acetate for 1 h. After dehydration in an acetone series, pellets were embedded in TAAB epoxy resin. Sections were stained with uranyl acetate and lead citrate. For serial reconstructions, blocks were trimmed to a minimal size to facilitate the identification of individual cells. Ribbons of sections were mounted on Formvar or Pioloform-coated slotted grids, then stained with uranyl acetate and lead citrate.

For freeze-fracture, cells fixed in tannic-glutaraldehyde as described above were washed thoroughly in buffer, frozen in slushed nitrogen, freeze fractured and shadowed with platinum and carbon in a Polaron freeze fracture station. Measurements of particle frequencies and sizes were taken from micrographs at a magnification of ×150000.

Reconstruction

Electron micrographs were taken of serially sectioned schizonts at magnifications of ×30000–60000 and further enlarged to ×150000 before being traced on to clear acetate sheets. The images were aligned according to 'best fit' considerations, using several position makers from adjacent regions of the infected red cell and surrounding structures. The images were either reconstructed manually on graph paper or were transferred via a digitized pad to a Kontron image processor running 3-dimensional reconstruction software. Sequences of 15–25 sections were used in these reconstructions and altogether 6 complete series were used for this study. These were supplemented with partial reconstructions of early stages of rhoptry development from 2 sequences of 6–10 serial sections.

RESULTS

Position of rhoptry genesis

As reported for other species of *Plasmodium* (Vickerman & Cox, 1967), merozoite apices are formed around the periphery of the schizont (Fig. 1A, B), commencing during and immediately after the final endomitotic divisions of the schizont stage. Towards the end of schizogony, the nuclear lobes lie close to the schizont's surface, spaced at regular intervals around its perimeter. The nuclear envelope remains intact during mitotic division (endomitosis), as in all the Apicomplexa. The terminal mitotic spindles (Fig. 1A) lie around the cell's periphery with their axes approximately parallel with the cell's surface. At both ends of each spindle, the spindle microtubules are inserted into an electron-dense mass (spindle pole body) occupying a nuclear pore (Fig. 2A). The axis of the spindle is generally tilted by about 70° (Fig. 1A) to the nuclear envelope at either end. The nuclear envelope bears ribosomes around most of its periphery, although not in the region of the spindle attachment (Fig. 2B, C). Peripheral to the spindle pole body, numerous free ribosomes and finely granular material are present within the cytoplasm (Fig. 2D).

Next, a thin layer of dense granular material begins to form an undercoating of the parasite's plasma membrane, defining the position of the future merozoite apex (Fig. 1A, B), and at the same time a cluster of coated vesicles, some of them in the process of budding from the outer nuclear membrane, appears to one side of the spindle pole body (Fig. 2A, D). Adjacent to this cluster a single large Golgi-like cisterna is formed, followed by rhoptries, micronemes and dense granules (Figs 2A and 3A–F). Small flat membranous vesicles come to lie close to the plasma membrane of the merozoite apex, extending beneath the plasma membrane to form the subplasmalemmal cisterna of the mature pellicle. A ring of dense granular material is formed just beneath the plasma membrane opposite the rhoptries, and the cisterna spreads out radially from this, leaving the central region free of cisternal membrane. The single dense ring eventually resolves into the 3 polar rings, and the plasma membrane is shaped into the elevated apical prominence (Fig. 3F). During these processes, 2 (or sometimes 3) parallel subpellicular microtubules (Fig. 4A) are assembled, their trajectory extending from the polar rings over the coated vesicle budding zone (Figs 3A, 4A and 6).

Golgi cisterna formation

The coated vesicle budding zone of the nuclear envelope consists of a distinct single cluster of up to

https://doi.org/10.1017/S0031182099006320 Published online by Cambridge University Press

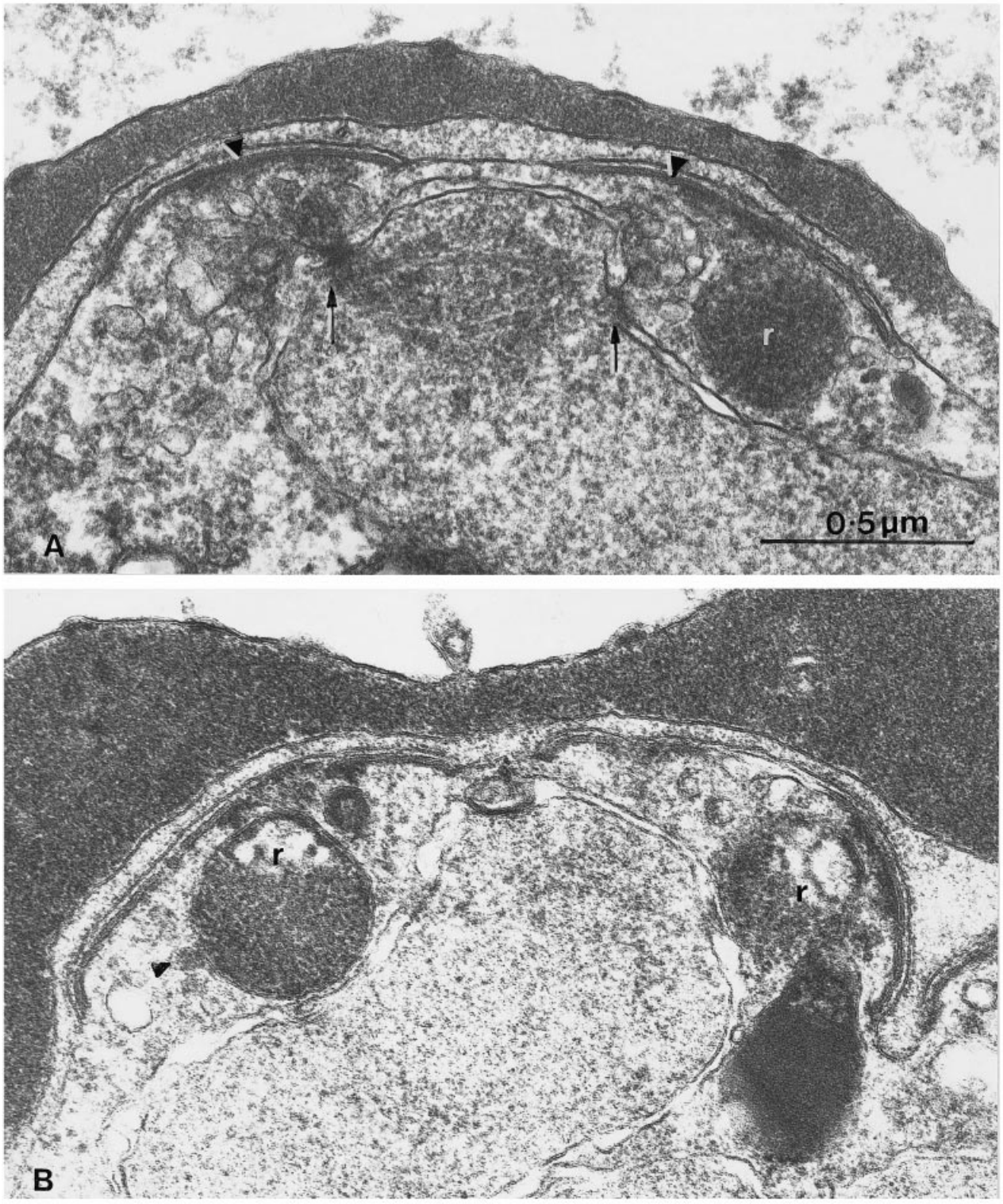

Fig. 1. Sections through early stages of merozoite formation, showing the relationship between the mitotic apparatus, the nucleus and the merozoite apices. (A) Terminal endomitotic spindle, with spindle pole bodies (arrows) inserted into a nuclear pore at each end. Opposite each spindle pole body is a focus of apical organelle formation, with the beginnings of a subpellicular cisterna (arrowheads), Golgi cisternae/vesicles and on the right of the micrograph, an early rhoptry (r). (B) Later stage, with clefts beginning to separate 2 merozoite apices containing developing rhoptries (r). Note the different degrees of development of the two rhoptries on the right of the micrograph, one loosely granular with a circular profile (above) and the other, immediately below it, showing the more mature, denser pear-shaped form. On the left there are indications of vesicular fusion at the periphery of one rhoptry (arrowhead). The magnifications of A and B are the same.

https://doi.org/10.1017/S0031182099006320 Published online by Cambridge University Press

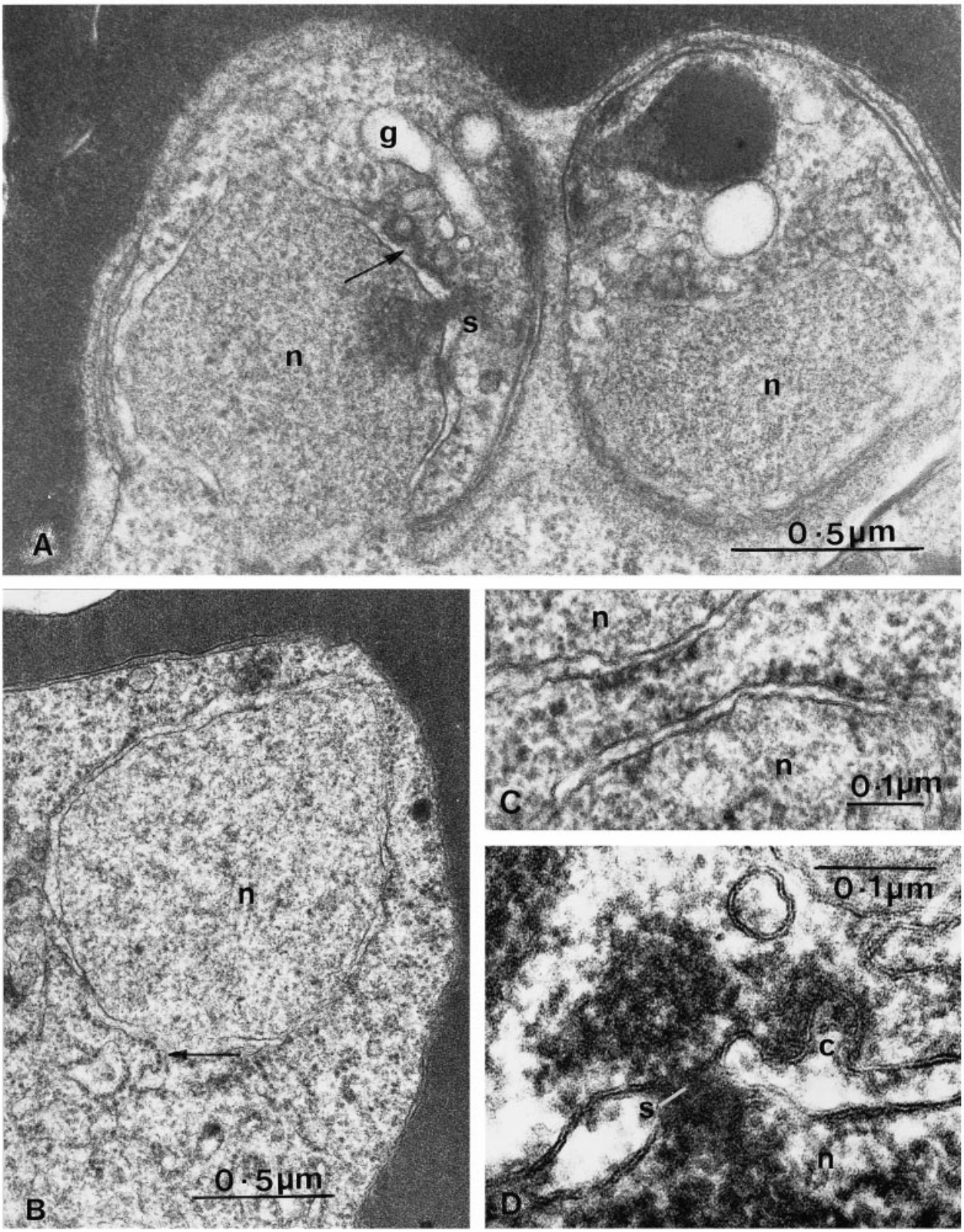

Fig. 2. (A) Section through 2 late-stage merozoite buds. The merozoite on the left shows the remains of a spindle and a prominent spindle pole body (s) passing through a nuclear pore; the nucleus (n) with a coated vesicle budding zone (arrow) and a single Golgi cisterna (g) are visible here. In the right hand merozoite the section has passed through a mature rhoptry, its duct pointing towards the apical prominence. (B) Nucleus (n) surrounded by rough endoplasmic reticulum in a late-stage schizont, with the nuclear envelope bearing numerous ribosomes, and the nuclear envelope continuous with the rough endoplasmic reticulum (arrow). (C) Section through parts of 2 juxtaposed nuclei (n) bearing clusters of ribosomes attached to their outer membranes. (D) Section through a spindle pole body (s) in early rhoptry formation, with a mass of dense granular material in the neighbouring cytoplasm and the end of the spindle within the nucleus (n). A coated vesicle (c) is seen to be budding from the outer nuclear membrane to the right of the spindle pole body.

https://doi.org/10.1017/S0031182099006320 Published online by Cambridge University Press

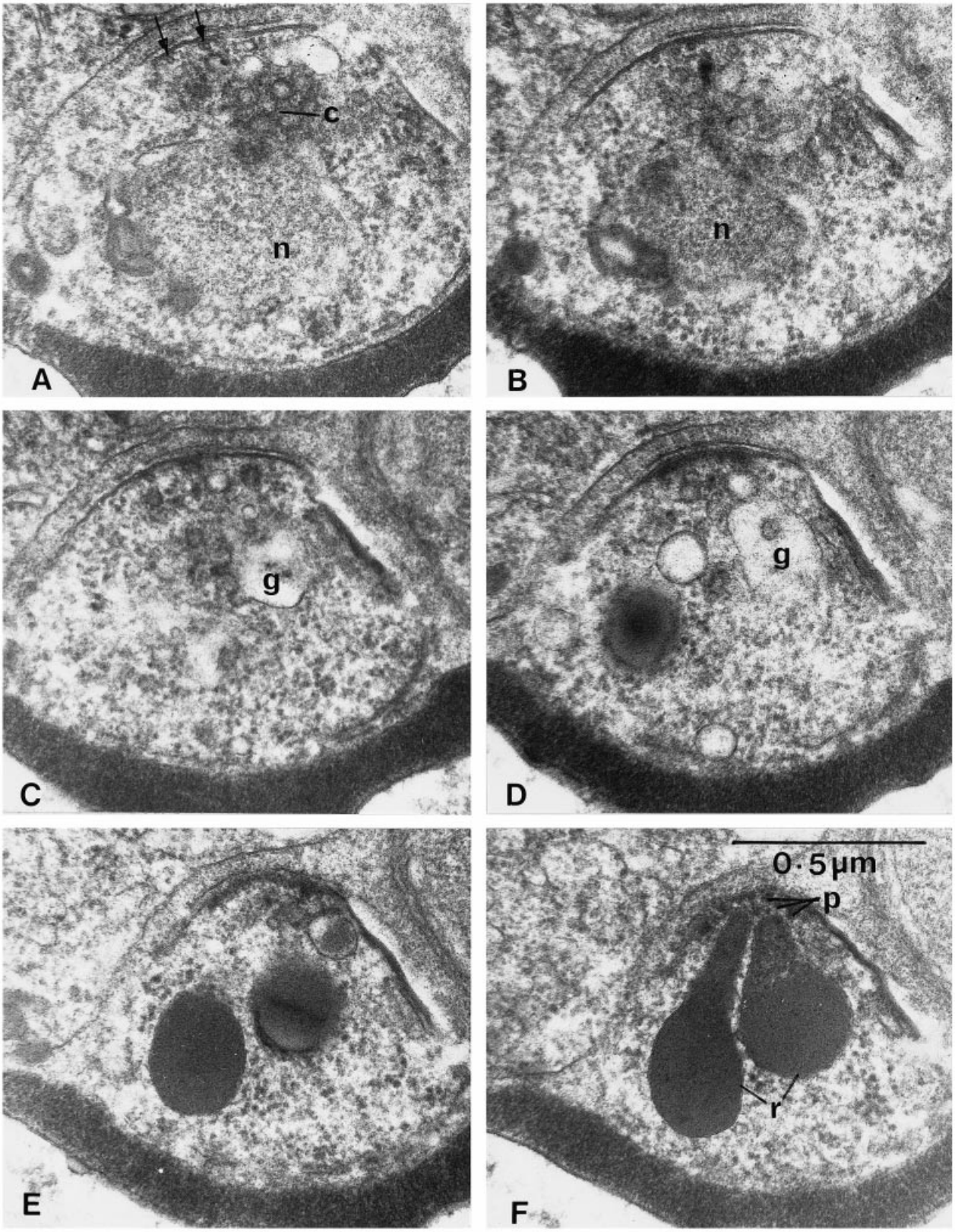

Fig. 3. (A–F) A sequence of 6 serial sections through the apical region of a budding merozoite showing the relationship between the nucleus (n), the coated vesicle budding zone (c), Golgi cisterna (g), rhoptries (r) and polar rings (p). Note the presence of a microtubule pair (arrows) beneath the pellicle. The series from which this sequence was selected was used to establish the 3-dimensional reconstruction shown in Fig. 6.

https://doi.org/10.1017/S0031182099006320 Published online by Cambridge University Press

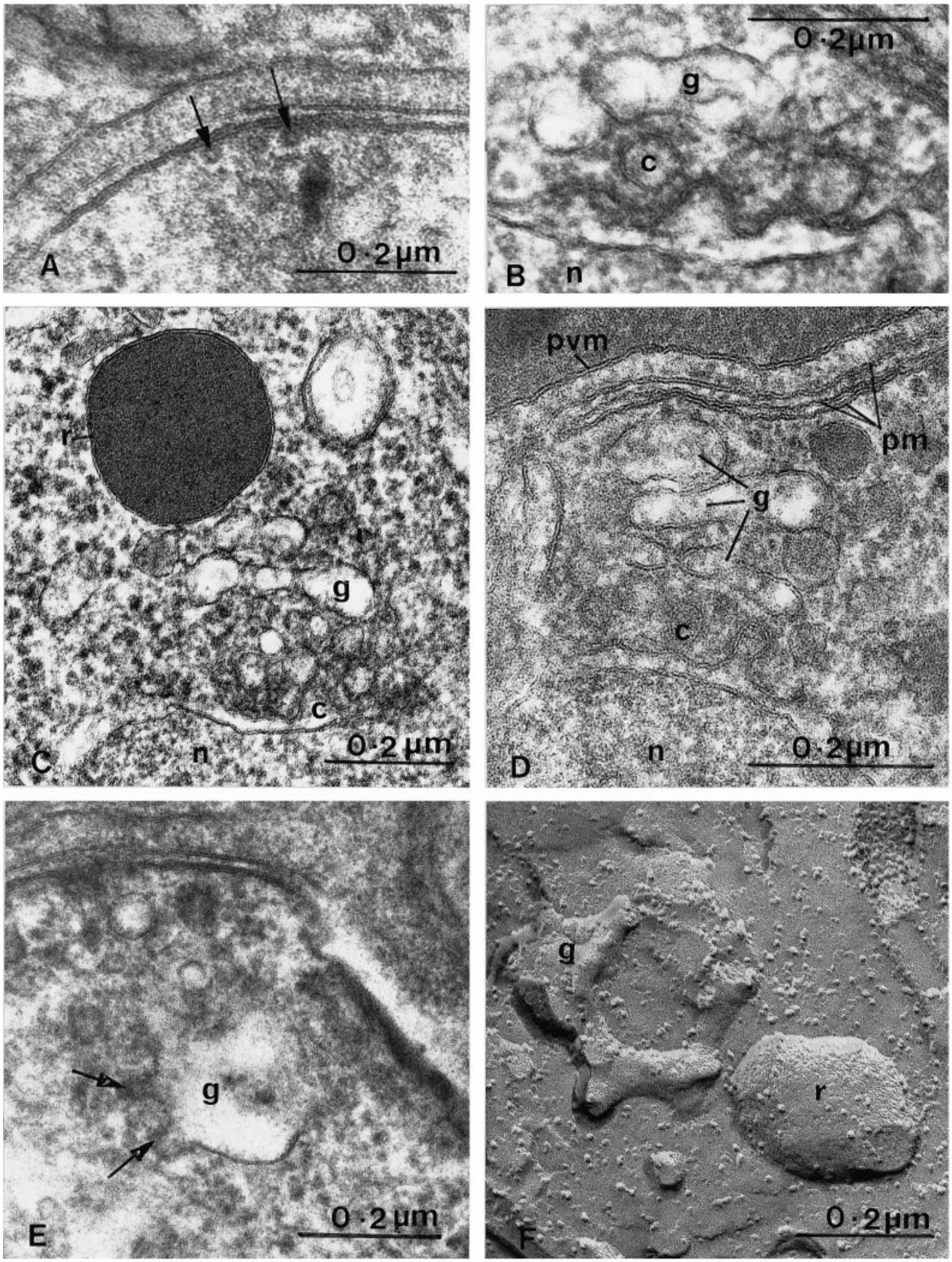

Fig. 4. (A) The subpellicular microtubule pair (arrows) shown in Fig. 3A, at higher magnification. (B) Detail of the coated vesicle budding zone (c) in an early merozoite showing coated vesicles budding from the outer nuclear envelope, and an overlying Golgi cisterna (g); the nucleus is below (n). (C–F) Details of the Golgi cisterna and associated structures; (C) shows part of the nucleus (n), a coated vesicle budding zone (c), a Golgi cisterna (g) and the base of a rhoptry (r), as well as other large and small vesicles. Similar structures are visible in (D), although here there are indications of a more complex Golgi apparatus, with 3 cisternal profiles; the 3 membranes of the merozoite

https://doi.org/10.1017/S0031182099006320 Published online by Cambridge University Press

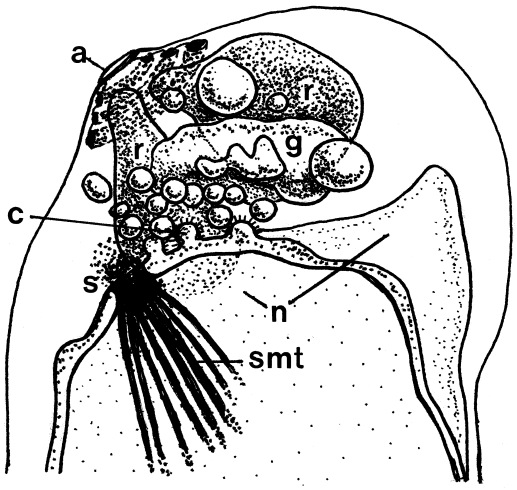

Fig. 5. A reconstruction of the apical ends of merozoites from sequences of 11 serial sections depicting the relationship between nucleus (n) with the residual spindle microtubules converging on the spindle pole body (s) inserted into a nuclear pore, the nuclear coated vesicle budding zone (c), Golgi cisterna (g) and rhoptries (r). The apical prominence (a) contains the 3 sets of polar rings (p).

20 vesicles (determined from serial sections) of uniform shape and diameter (about 50 nm) and bearing bristly coats (Figs 2A, D, 3A, 4B–D, 5 and 6). Adjacent to this vesicular cluster and sited closer to the parasite's surface is situated a single, or in rare instances 2 large smooth walled flattened cisterna (Fig. 4D). Reconstructions from serial sections (Figs 5 and 6) confirm its single cisternal nature and shows that it is highly variable in form, being variously a flat or concave discoidal structure 330–500 nm in diameter. Rarely, 3 cisternae were found, one larger than the others (see Fig. 4D), or the cisterna took the form of a convoluted tubular sac (not shown).

The perimeter of the cisterna typically bears a few small protrusions with bristly exteriors similar to those of coated vesicles (Figs 3C, 4E and 6). These protrusions are also seen clearly in freeze-fractured specimens (Fig. 4F). More peripherally towards the parasite's surface is a further cluster of vesicles, of 2 sizes: (1) small (40 nm diameter) vesicles, some of them bearing bristly coats, and (2) much larger smooth elliptical, rounded or irregularly shaped vesicles in the range 85–230 nm (Figs 7A and 8C). The vesicle–cisterna complex appears at the earliest stage of rhoptry formation, and disappears only after the merozoite has separated from the residual body.

Rhoptry formation

In our study, the sequence of rhoptry development was determined in random sections from more than 50 schizonts of different stages of maturation, and in 17 sets of serial sections of budding merozoites (Figs 7A–G and 8A–C). The extent of general merozoite assembly and budding was taken to indicate the stage of development in this analysis. Rhoptries were first detected as small vesicles with a circular profile, about 150 nm in diameter situated between the nuclear envelope and the plasma membrane of the schizont (Jaikaria *et al*. 1993), close to the cluster of *trans*-Golgi vesicles. These early rhoptries contain a loosely packed matrix of 5–8 nm granules. Small (about 40 nm) vesicles are present on the juxta-

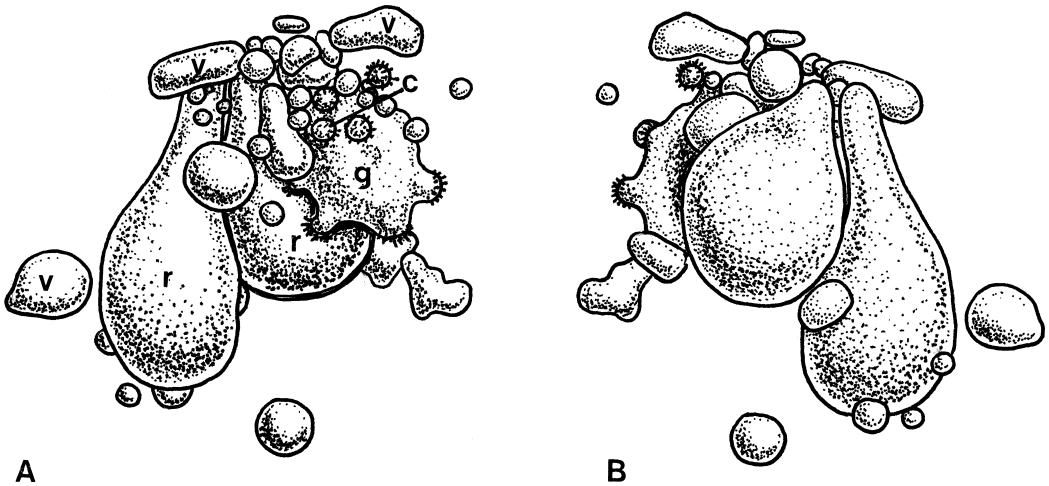

Fig. 6. (A and B) The views at 180° of a reconstruction of the complex of coated vesicle, Golgi cisterna and rhoptries, derived from a series of 9 serial sections in a developing merozoite; 6 of these sections are depicted in Fig. 3. c, Nucleus-derived coated vesicle cluster; g, Golgi cisterna with other coated vesicles budding off around its margin; r, rhoptry; v, other vesicles of various sizes.

pellicle are also visible (pm). (E) A section cut parallel to the main plane of the Golgi cisterna (detail from Fig. 3C), showing coated vesicle formation (arrows) around the perimeter of the Golgi cisterna (g). (F) A similar Golgi cisterna (g) and a rhoptry (r) in a freeze-fractured specimen. Note the presence of intramembranous particles in the cytoplasm-facing surfaces of the fractured membranes of both organelles.

https://doi.org/10.1017/S0031182099006320 Published online by Cambridge University Press

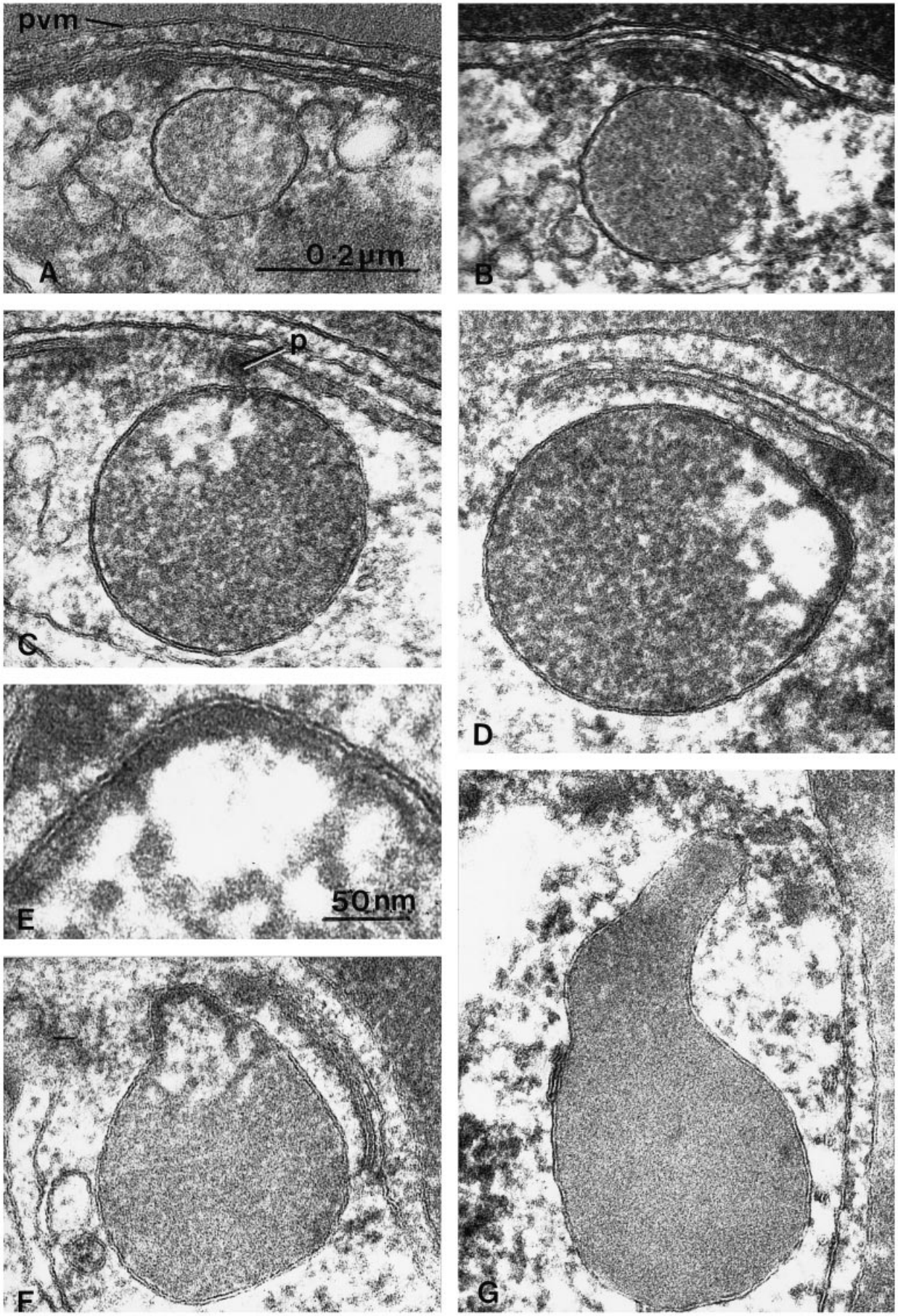

Fig. 7. For legend see opposite.

https://doi.org/10.1017/S0031182099006320 Published online by Cambridge University Press

nuclear aspect of these spheroidal rhoptries, and both sectioned and freeze-fractured material show vesicles which appear to be fusing with the rhoptry base and sides (Figs 1B and 9C). As the rhoptry grows in diameter, its contents eventually become more closely packed, and when mature the rounded base is almost filled with a mass of dense granules (Fig. 8B).

The first sign of duct development appears in rhoptries with diameters of about 350 nm in the region facing obliquely towards the schizont surface, with an electron-lucent area appearing at the end closest to the developing polar rings (Fig. 7C). In a slightly later stage, the rhoptry surface in this region is distorted into a low conical projection (Fig. 7D). The membrane of this part of the rhoptry gains a dense undercoating which persists as an apical cap on the growing duct (Fig. 7D, E), and the internal matrix consists of cords of finely granular or flocculent appearance with lucent gaps between. Thereafter this region extends progressively from the basal bulb to form a rhoptry duct up to 240 nm long, conferring a pear-shaped profile on the mature organelle (Fig. 10).

During this second phase of rhoptry development, the duct frequently assumes rather bizarre shapes with irregular bulges or bends along its length (Fig. 7G). Eventually the tip of the growing rhoptry duct comes into close proximity with the central area of the merozoite's apical prominence, and the long axis of the rhoptry is now orientated approximately parallel to that of the merozoite (Fig. 11D). In all the specimens examined, the tips of the two rhoptries remained separate from each other into maturity, although a single small (about 8 nm) vesicle was often observed where their tips converged on the membrane of the apical prominence (not shown). No central microtubules could be convincingly identified in association with the rhoptry duct in *P. falciparum*.

Within the basal region of the rhoptry the matrix becomes very densely packed, and the apparent granule size decreases from a maximum of 8 nm to about 4 nm (Fig. 7D, F, G). In contrast, the interior of the rhoptry duct alters considerably during development, beginning as a heterogenous matrix of jumbled material resembling loosely packed irregular vesicles (Fig. 8A), but becoming more closely packed until, when mature, they present a dense, finely granular appearance (Fig. 8B). No lamellar configurations such as those described in tannic acid-fixed merozoites of *P. falciparum* (Stewart, Schulman & Vanderberg, 1986) or *P. knowlesi* (Bannister *et al.* 1986) were detected, but freeze-fractured rhoptry ducts showed some signs of a heterogenous matrix internally (Fig. 9A).

As the duct elongates, a line of vesicles (diameter 40 nm) is present in the region between the Golgi cisterna and the duct's apex, suggesting the flow of vesicular traffic from the former to the latter (Fig. 8C) although no instances of actual fusion were found.

In all parasites examined, including serially sectioned material, 1 rhoptry was seen to have begun formation and to mature before the other (see Fig. 1B). Occasionally, an additional dense spheroidal mass resembling the basal bulb of an immature third rhoptry was found in association with a mature rhoptry pair.

Rhoptry membrane

In section, each rhoptry is surrounded by a 7 nm-thick unit membrane (Fig. 8A–C). In freeze-fractured and freeze-etched material (Figs 4F and 9A–D) the 2 fracture faces of the rhoptry membrane show distinctive populations of intramembranous particles (IMPs). In a limited number (10) of rhoptries examined, the IMPs exposed on the concave fracture surface of the outer membrane leaflet (i.e. facing the interior of the rhoptry) had a frequency of 1070–2241/μm^2 and had diameters of about 12 nm, with a small number of larger (16 nm) IMPs. The IMPs of the convex surface of the leaflet adjacent to the rhoptry interior were fewer (569–903/μm^2) but predominantly larger (14–16 nm) than on the apposed surface of the membrane, with a few smaller (10–12 nm) IMPs in the population; occasional rod-like IMPs measuring 24 × 10 nm also occurred on this face. Many of the 14–16 nm particles showed central depressions (Fig. 9B).

There were no signs of regional differences between the basal and duct regions of rhoptries, although in some cases both P and E faces have areas

Fig. 7. (A–G) Details of rhoptry formation during merozoite development. (A and B) Small, early rhoptries with granular interiors, surrounded by small vesicles; the 3 membranes of the merozoite pellicle are visible, with the parasitophorous vacuole membrane (pvm) above them. In (C) the rhoptry has increased in size and an electron-lucent region has appeared in the region closest to the forming apical prominence where the polar rings are beginning to form (p) and the inner pellicular membranes are absent within the ring (arrow). In (D) the apical end of the rhoptry has begun to develop a rhoptry duct, first seen as a bulge at its apical end (right); here the rhoptry membrane has a dense undercoating, shown in more detail in (E), where the reticular interior of this region is also depicted. In (F) the rhoptry duct has lengthened and the granular material of the basal part has become more tightly packed. In (G) this process has proceeded further and the rhoptry duct is also more electron-dense, although clearly different in composition from the basal part of the rhoptry. The magnifications of (B–D) and (F, G) are the same as in (A).

https://doi.org/10.1017/S0031182099006320 Published online by Cambridge University Press

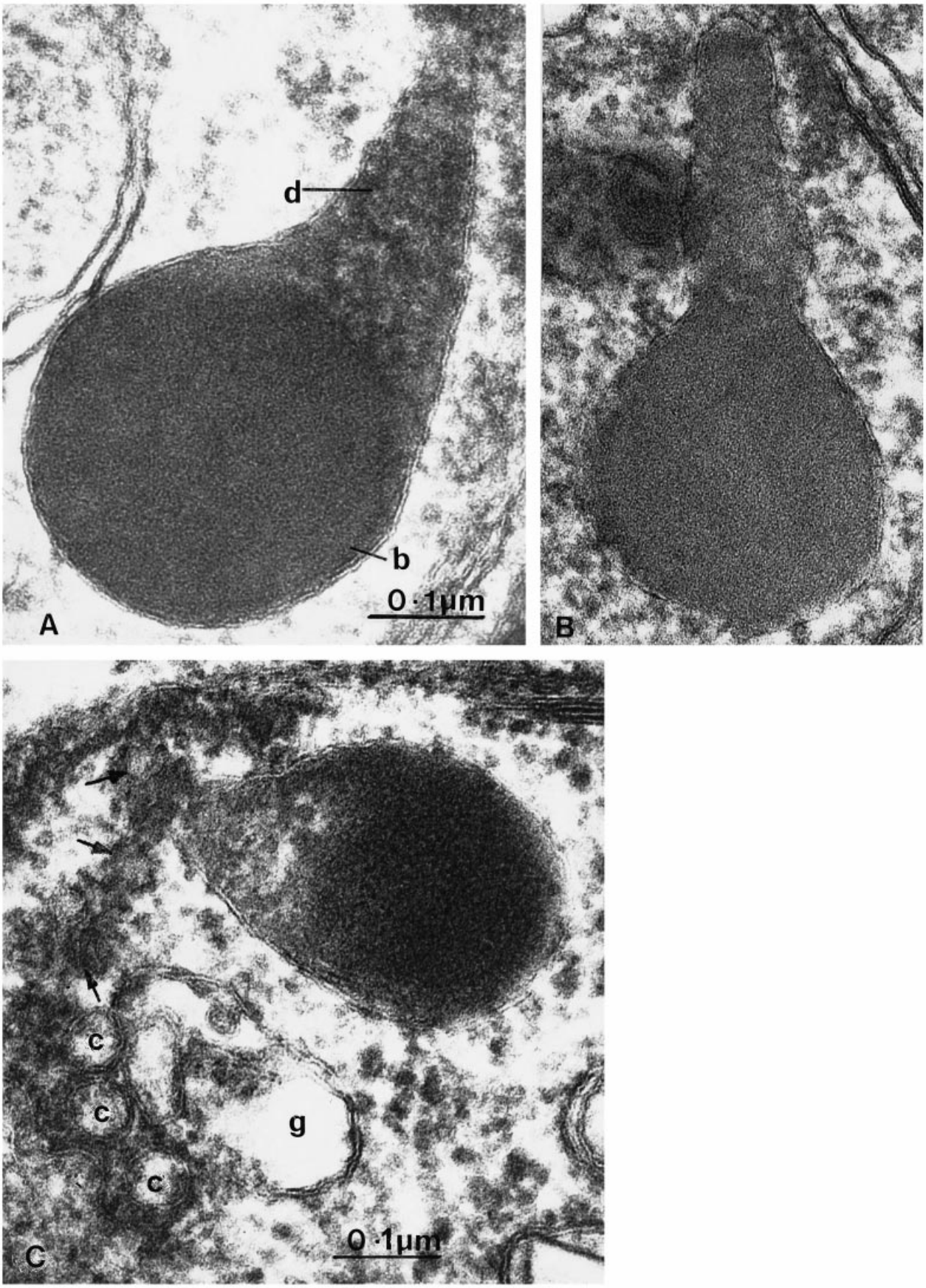

Fig. 8. (A–C) Details of rhoptry development. (A and B) Two later stages in rhoptry maturation. In (A) the rhoptry duct (d) is full length, although its shape is not fully mature. The loose, reticular appearance of the rhoptry duct is clearly quite distinct from the spheroidal basal region (b), which is now densely packed and coherent. In (B), in the fully mature state, the duct contents have attained a finely granular/fibrillar texture, and the duct is now relatively narrow. In (C) there are indications of vesicular traffic from the coated vesicle budding zone of the nucleus (c) to the Golgi cisterna (g) and thence by smaller dense coated vesicles (arrows) to the rhoptry duct tip.

https://doi.org/10.1017/S0031182099006320 Published online by Cambridge University Press

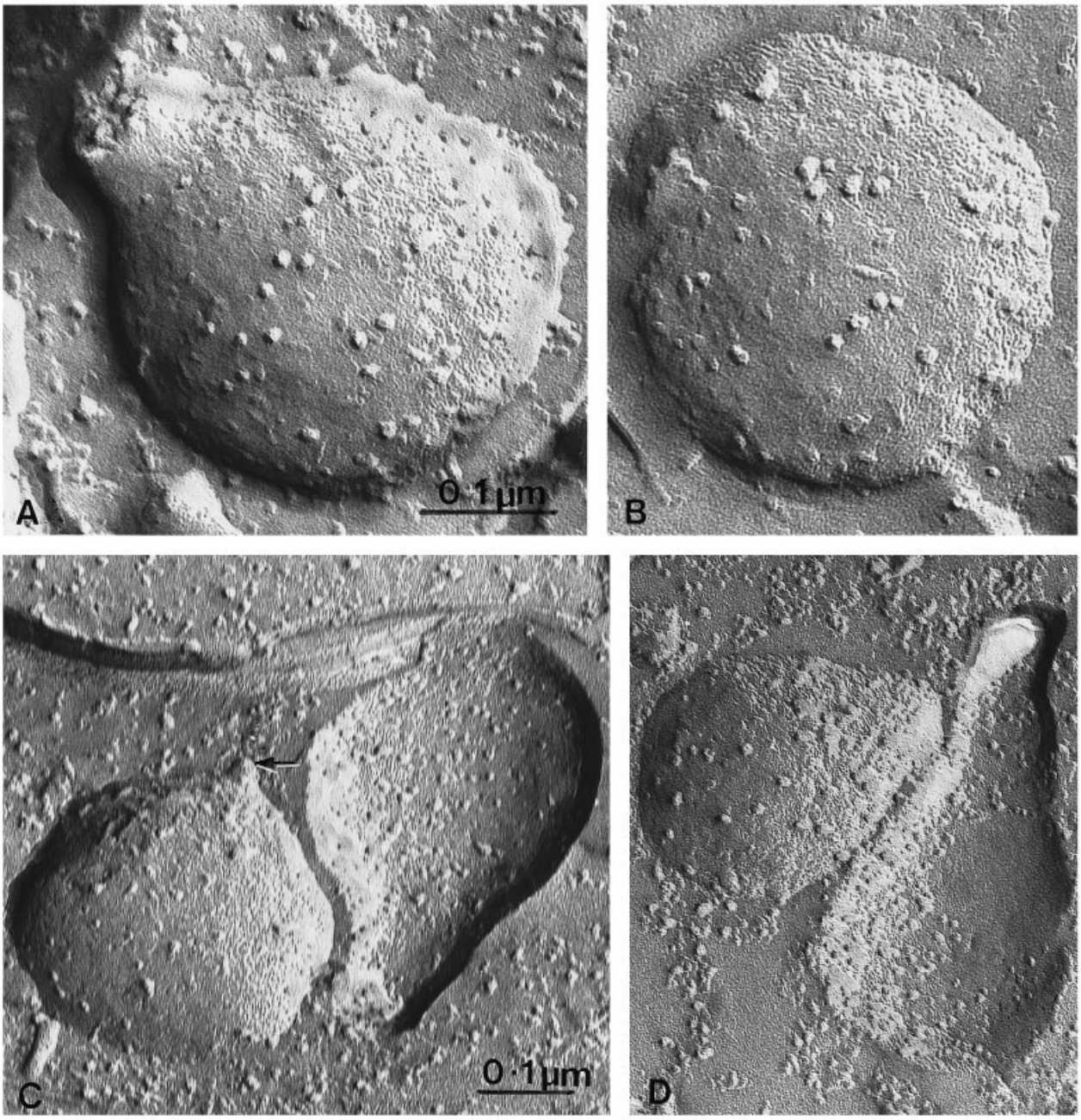

Fig. 9. Freeze-fracture replicas of developing rhoptries, showing the distribution of intramembrane particles in their membranes. (A) A maturing rhoptry with a short duct which has been fractured across apically to show the complex texture of its interior. Note the variety of large, small and rod-shaped IMPs in the cytoplasm-facing fracture face of its membrane. (B) Basal end of a developing rhoptry, with the cytoplasm-facing fracture face exposed; IMPs of different sizes and rod-shaped IMP are visible. (C) Two rhoptries, one more advanced than the other, and with different fracture faces visible; the younger, more rounded rhoptry (left) shows the externally-facing fracture face with large IMPs, and the other (right) reveals the fracture surface facing the rhoptry interior, with smaller but more homogenous IMP sizes; a likely instance of vesicle fusion with the rhoptry base is indicated by an arrow. (D) Another pair of rhoptries, the rounded one to the left being again less advanced than that on the right showing a rhoptry duct. The left fractured rhoptry is convex in this replica, and the right one is concave, revealing, respectively fracture surfaces facing the rhoptry exterior and interior. Areas of particle-free membrane are visible on the right-hand rhoptry. Note that (C) and (D) are oriented in opposite directions: the merozoite apex is at the bottom of (C) and the top of (D) in order that the direction of shadowing is the same in both replicas. The magnifications for (B), (C) and (D) are as in (A).

https://doi.org/10.1017/S0031182099006320 Published online by Cambridge University Press

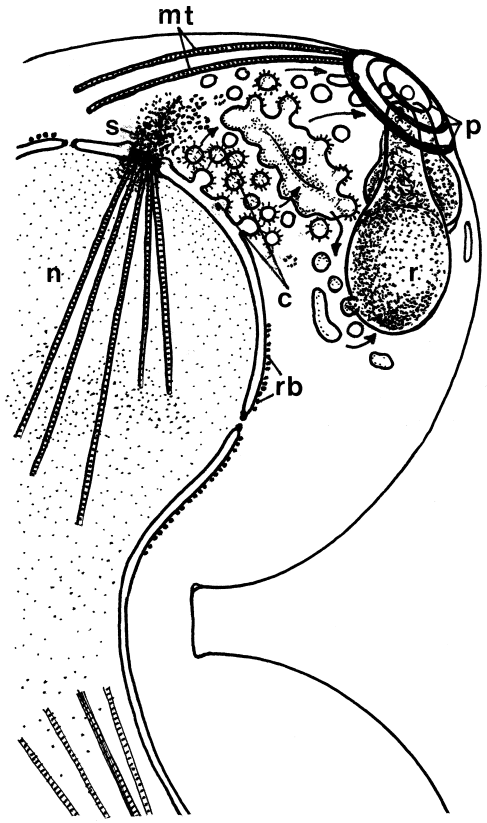

Fig. 10. A diagram summarizing the spatial relationships of the coated vesicle budding zone (c) of the nucleus (n), the spindle pole body (s) with attached microtubules within the nucleus, the Golgi cisterna (g), rhoptries (r) and polar rings around the apical prominence in a merozoite bud. The arrows indicate the proposed routes of vesicle trafficking within the coated vesicle-rhoptry complex to the basal and apical ends of the rhoptries. Also shown are the band of subpellicular microtubules (mt) and ribosomes attached to the nuclear envelope (rb).

of particle-free membrane (Fig. 9C). Small vesicular extensions of the rhoptry base suggest the fusion of small vesicles with this structure (Fig. 9C).

DISCUSSION

Site of rhoptry formation

Our results agree with the conclusions of Aikawa, Huff & Sprinz (1967) for *P. elongatum*, and Shaw & Tilney (1992) for *Theileria* that the anterior poles of new merozoites and their contents are closely related to the spindle pole bodies of the final division spindle. Hence, merozoite apices are paired, one at each end of each terminal mitotic spindle (Fig. 10). The spindle pole body's proximity to the zone of coated vesicle budding suggests that it (or some related entity) initiates the formation of the apical secretory organelles, as well as the synthesis of cytosolic proteins by the cluster of ribosomes which accumulate at this locus.

Route of protein targeting to rhoptries

The association of rough endoplasmic reticulum, nuclear envelope and vesicle budding zone are similar to those proposed as a site of protein synthesis and targeting to the apical organelles in *Toxoplasma* (Hager *et al*. 1999). Vesicle budding from the nuclear envelope has also been indicated previously in merozoites of *P. falciparum* (Langreth *et al*. 1978) and *P. knowlesi* (cited by Ward *et al*. 1994), and in sporozoite formation in *P. berghei* (Schrével, Asfaux-Foucher & Bafort, 1977) and may be characteristic of invasive stages in apicomplexans as a group. Preliminary evidence also indicates that at least one of the rhoptry proteins (RAP-1) immunolocalizes to the nuclear envelope during development (L. H. Bannister and R. E. Fowler, unpublished observations).

The Golgi body

Although inhibition of rhoptry protein processing by brefeldin implies a Golgi body in the secretory pathway, there has been much debate about the existence of true Golgi bodies in *Plasmodium* erythrocytic stages (Haldar & Holder, 1993; Banting, Benting & Lingelbach, 1995; van Wye *et al*. 1996). The candidate Golgi bodies in trophozoites, detected by immunolabelling with the Golgi marker rab6 (van Wye *et al*. 1996) are tubulo-vesicular structures, and appear to be rather different in organization from those of nascent merozoites, described in the present paper, although there is developmental continuity between the two (L. H. Bannister and J. M. Hopkins, unpublished observation). Our results show the early merozoite Golgi body to be a single discoidal cisterna, receiving small vesicles at its *cis*-face from the nuclear envelope, and budding off around its perimeter vesicles of various shapes and sizes destined to form membranous organelles of the merozoite apex and pellicle. The single cisterna Golgi body of the *P. falciparum* merozoite clearly differs from the multi-cisternal Golgi body of *Toxoplasma* (Shaw, Roos & Tilney, 1998), but its relation to the nuclear membrane-derived vesicles and other vesicular structures appears to be identical.

Segregation of basal and duct rhoptry regions

The immuno-electron microscopical data of Bushell *et al*. (1988), Ingram *et al*. (1988) and Crewther *et al*. (1990) showed that RAP-1 is exclusively localized to the rhoptry base, while AMA-1 is confined to the apical duct, as also are the 225 kDa rhoptry protein (Roger *et al*. 1988) and the 140/130/110 kDa rhoptry protein complex (Sam-Yellowe *et al*. 1995), a remarkable occurrence considering that they are contained within a single bounding membrane. This

https://doi.org/10.1017/S0031182099006320 Published online by Cambridge University Press

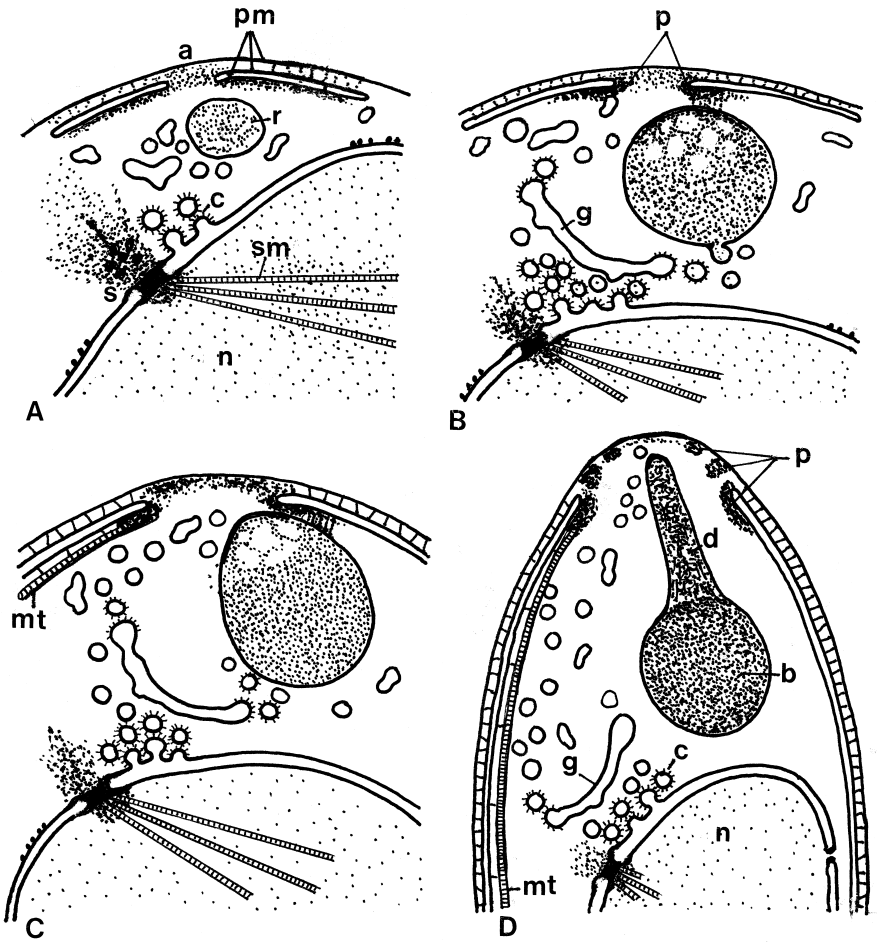

Fig. 11. (A–D) A sequence of diagrams depicting the origins and development of rhoptries in *Plasmodium falciparum* from the earliest appearance of a small rhoptry vesicle to the mature state within a late stage merozoite bud. a, Apical pole of the future merozoite; b, basal end of the rhoptry; c, coated vesicle budding zone; d, rhoptry duct; g, Golgi cisterna; mt, subpellicular microtubules; n, nucleus; p, polar rings or polar ring precursors; pm, 3 membranes of the pellicle, including the parasite plasma membrane and the 2 underlying membranes of the subplasma membrane cisterna; r, rhoptry; s, spindle pole body; sm, spindle microtubules.

prompts 2 questions: how do the proteins reach these 2 domains, and how do they remain in them rather than intermingling by diffusion?

Our structural evidence suggests that the rhoptry grows initially by progressive fusion of small Golgi-derived vesicles at its perimeter to form a spheroidal mass, from which the duct later extends partly by some external shaping process and perhaps also by vesicle fusion at its apex. When the incipient rhoptry duct is first detected as a low conical projection, the rhoptry interior is clearly divided into 2 regions: (1) a basal uniformly granular mass, and (2) a more apical region with electron-lucent areas between cords composed of smaller granules. Jaikara *et al.* (1993) reported that RhopH-3 (the 110 kDa duct protein) is synthesized and transported to early rhoptry vesicles before RAP-1 (which eventually occupies the rhoptry base). This would suggest that after they entered the early rhoptry, duct proteins co-aggregate and are displaced towards the rhoptry apex by other types of protein delivered by vesicular fusion at the basal end. At the same time, more protein may be added at the duct apex by further, differential vesicle delivery to increase the size of this part of the rhoptry and its complexity. The mechanisms of vesicle delivery to the rhoptry are not clear. The rhoptry base is close to the Golgi cisterna, and vesicles could reach it by random diffusion, but some more vectorial system carrying vesicles to the duct tip, e.g. along microtubules, may be present (although we have not found evidence of close contact or structural links between subpellicular microtubules and rhoptry-related vesicles).

During the later stages of rhoptry maturation, there is a great increase in internal density, pointing to the removal of water and co-aggregation of its proteins, as also found in other secretory vesicles, e.g. zymogen granules in mammalian pancreatic acini (see Goncz, Behrsing & Rothman, 1995). These processes could also ensure the maintenance of distinctive basal and duct protein populations by differential co-aggregation caused, e.g. by non-covalent complex formation, as occurs between the basally situated proteins RAP-1 and RAP-2 (Bushell

https://doi.org/10.1017/S0031182099006320 Published online by Cambridge University Press

et al. 1988; Howard & Reese, 1990; Ridley *et al*. 1990; Saul *et al*. 1992), and also between the 3 duct proteins RhopH1-3 (140/130/110 kDa). It is interesting that *Toxoplasma* rhoptries become acidified as they mature (Shaw *et al*. 1998), since a lowering of pH causes aggregation of pancreatic acinar proteins *in vitro* (Dartsch, Kleene & Kern, 1998). Such a process might explain the transition to a tightly packed internal structure in developing rhoptries.

The above considerations apply to the proteins of rhoptries, but these organelles may also contain substantial amounts of lipidic material. Evidence for a lipid presence includes: (1) fluorescent lipid probes are incorporated into the *P. falciparum* merozoite apex and thence into the parasitophorous vacuole during invasion (Mikkelsen *et al*. 1998); (2) RhopH-3 is more susceptible to trypsin after phospholipase treatment, indicating a lipid association (Etzion *et al*. 1991); and (3) *Toxoplasma* rhoptries have a 26% lipid content (Foussard, Leriche & Dubremetz, 1991). As yet, lipids (or lipid precursors) have not been identified ultrastructurally within rhoptries, but they may be of relatively low molecular weight, and unless in salt form, are likely to be depleted by non-polar solvents used in preparation for electron microscopy. The electron-lucent apical regions of the early rhoptries and minor electron-lucent components of the early rhoptry neck may therefore be areas from which lipid has been extracted, although lipid may become complexed intimately with proteins as rhoptries mature and therefore indistinguishable in sectioned material.

The rhoptry membrane

On the basis of our freeze-fracture results, at least four morphologically distinct classes of IMPs are present in the rhoptry membrane, distributed over both basal and apical parts of the rhoptry, and asymetrically arranged within the membrane bilayer. The functions of the IMPs and other membrane proteins which may be present await further investigation, although activities such as ionic and water regulation as well as Golgi vesicle and microneme docking and fusion can be predicted. It is significant that the larger IMPs show central depressions indicating central pores, suggesting they might be transport channels.

The high IMP frequency also indicates a substantial protein presence within the rhoptry membrane, which must contribute to the numerous rhoptry protein classes reported for this organelle (see Etzion *et al*. 1991). It is worth reflecting that not all rhoptry proteins are located in the interior or are likely to be secreted during invasion. However, such proteins are likely to be crucial to the maturation of rhoptries, and merit further investigation, e.g. as potential targets for ion transport blockade.

We thank Dr Tony Brain for freeze-fracturing the specimens, and Dr Anton Dluzewski, Miss C. O'Shaughnessy and Miss R. E. Fookes for facilitating provision of parasite cultures. The study was supported by the Wellcome Trust (grant numbers 037082 and 048244) and the Special Trustees of St Thomas' and of Guy's Hospital to whom the authors are much indebted. S. K. is a Wellcome Trust Senior Research Fellow in Clinical Science. We also wish to thank the staff of the Electron Microscope Unit, Guy's Hospital, for their continuing and much appreciated assistance.

REFERENCES

AIKAWA, M., HUFF, C. G. & SPRINZ, H. (1967). Fine structure of the asexual stages of *Plasmodium elongatum*. *Journal of Cell Biology* **34**, 229–249.

BANNISTER, L. H. & DLUZEWSKI, A. R. (1990). The ultrastructure of red cell invasion in malaria infections: a review. *Blood Cells* **16**, 257–292.

BANNISTER, L. H. & MITCHELL, G. H. (1989). The fine structure of secretion by *Plasmodium knowlesi* merozoites during red cell invasion. *Journal of Protozoology* **36**, 362–367.

BANNISTER, L. H. & MITCHELL, G. H. (1995). The role of the cytoskeleton in *Plasmodium falciparum* merozoite biology: an electron-microscopic view. *Annals of Tropical Medicine and Parasitology* **89**, 105–111.

BANNISTER, L. H., MITCHELL, G. H., BUTCHER, G. A. & DENNIS, E. D. (1986). Lamellar membranes associated with rhoptries in erythrocytic merozoites of *Plasmodium knowlesi*: a clue to the mechanism of invasion. *Parasitology* **92**, 291–303.

BANTING, G., BENTING, J. & LINGELBACH, K. (1995). A minimalist view of the secretory pathway in *Plasmodium falciparum*. *Trends in Cell Biology* **5**, 340–343.

BUSHELL, G. R., INGRAM, L. T., FARDOULYS, C. A. & COOPER, J. A. (1988). An antigenic complex in the rhoptries of *Plasmodium falciparum*. *Molecular and Biochemical Parasitology* **28**, 105–112.

CREWTHER, P. E., CULVENOR, J. G., SILVA, A., COOPER, J. A. & ANDERS, R. F. (1990). *Plasmodium falciparum*: two antigens of similar size are located in different compartments of the rhoptry. *Experimental Parasitology* **70**, 193–206.

DARTSCH, H., KLEENE, R. & KERN, H. F. (1998). *In vitro* condensation-sorting of enzyme proteins isolated from rat pancreatic acinar cells. *European Journal of Cell Biology* **75**, 211–222.

DLUZEWSKI, A. R., LING, I. T., RANGACHARI, K., BATES, P. A. & WILSON, R. J. M. (1984). A simple method for isolating viable mature parasites of *Plasmodium falciparum* from cultures. *Transactions of the Royal Society of Tropical Medicine and Hygiene* **78**, 622–624.

ETZION, Z., MURRAY, M. C. & PERKINS, M. E. (1991). Isolation and characterization of rhoptries of *Plasmodium falciparum*. *Molecular and Biochemical Parasitology* **47**, 51–61.

FOUSSARD, F., LERICHE, M. A. & DUBREMETZ, J. F. (1991). Characterization of the lipid content of *Toxoplasma gondii* rhoptries. *Parasitology* **102**, 367–370.

GONCZ, K. K., BEHRSING, R. & ROTHMAN, S. S. (1995). The protein content and morphogenesis of zymogen granules. *Cell and Tissue Research* **280**, 519–530.

HAGER, K. M., STRIEPEN, B., TILNEY, L. G. & ROOS, D. (1999). The nuclear envelope serves as an intermediary between the ER and Golgi complex in the intracellular parasite *Toxoplasma gondii*. *Journal of Cell Science* **112**, 2631–2638.

HALDAR, K. & HOLDER, A. A. (1993). Export of parasite proteins to the erythrocyte in *Plasmodium falciparum*-infected cells. *Seminars in Cell Biology* **4**, 345–353.

HOWARD, R. F. & REESE, R. T. (1990). *Plasmodium falciparum*: hetero-oligomeric complexes of rhoptry polypeptides. *Experimental Parasitology* **71**, 330–342.

HOWARD, R. F. & SCHMIDT, C. M. (1995). The secretory pathway of *Plasmodium falciparum* regulates transport of Pf82/RAP-1 to the rhoptries. *Molecular and Biochemical Parasitology* **74**, 43–54.

HOWARD, R. F., NARUM, D. I., BLACKMAN, M. & THURMAN, J. (1998). Analysis of the processing of *Plasmodium falciparum* rhoptry-associated protein-1 and localization of Pr86 to schizont rhoptries and p67 to free merozoites. *Molecular and Biochemical Parasitology* **92**, 111–122.

INGRAM, L. T., STENZEL, D. J., KARA, U. A. & BUSHELL, G. R. (1988). Localisation of internal antigens of *Plasmodium falciparum* using monoclonal antibodies and colloidal gold. *Parasitology Research* **74**, 208–215.

JAIKARIA, N. S., ROZARIO, C., RIDLEY, R. G. & PERKINS, M. E. (1993). Biogenesis of rhoptry organelles in *Plasmodium falciparum*. *Molecular and Biochemical Parasitology* **57**, 269–279.

LAMBROS, C. & VANDERBERG, J. P. (1979). Synchronization of *Plasmodium falciparum* erythrocytic stages in culture. *Journal of Parasitology* **65**, 418–420.

LANGRETH, S. G., JENSEN, J. B., REESE, R. T. & TRAGER, W. (1978). Fine structure of human malaria in vitro. *Journal of Protozoology* **25**, 443–452.

MIKKELSEN, R. B., KAMBER, M., WADWA, K. S., LIN, P.-S. & SCHMIDT-ULLRICH, R. (1988). The role of lipids in *Plasmodium falciparum* invasion of erythrocytes: A coordinated biochemical and microscopic analysis. *Proceedings of the National Academy of Sciences, USA* **85**, 5956–5960.

OGUN, S. A. & HOLDER, A. A. (1994). *Plasmodium yoelii*: brefeldin A-sensitive processing of proteins targeted to the rhoptries. *Experimental Parasitology* **79**, 270–278.

PERKINS, M. E. (1992). Rhoptry organelles of apicomplexan parasites. *Parasitology Today* **8**, 28–32.

READ, M., SHERWIN, T., HOLLOWAY, S. P., GULL, K. & HYDE, J. E. (1993). Microtubular organization visualized by immunofluorescence microscopy during erythrocytic schizogony in *Plasmodium falciparum* and investigation of post-translational modifications of parasite tubulin. *Parasitology* **106**, 223–232.

RIDLEY, R. G., TAKACS, B., LAHM, H. W., DELVES, C. J., GOMAN, M., CERTA, U., MATILE, H., WOOLLETT, G. R. & SCAIFE, J. G. (1990). Characterisation and sequence of a protective rhoptry antigen from *Plasmodium falciparum*. *Molecular and Biochemical Parasitology* **41**, 125–134.

ROGER, N., DUBREMETZ, J. F., DELPLACE, P., FORTIER, B., TRONCHIN, G. & VERNES, A. (1988). Characterization of a 225 kilodalton rhoptry protein of *Plasmodium falciparum*. *Molecular and Biochemical Parasitology* **27**, 135–141.

SAM-YELLOWE, T. Y., FUJIOKA, H., AIKAWA, M. & MESSINEO, D. G. (1995). *Plasmodium falciparum* rhoptry proteins of 140/130/110 kd (Rhop-H) are located in an electron lucent compartment in the neck of the rhoptries. *Journal of Eukaryotic Microbiology* **42**, 224–231.

SAUL, A., COOPER, J., HAUQUIST, D., IRVING, D., CHENG, Q., STOWERS, A. & LIMPABOON, T. (1992). The 42 kilodalton rhoptry-associated protein of *Plasmodium falciparum*. *Molecular and Biochemical Parasitology* **50**, 139–150.

SCHRÉVEL, J., ASFAUX-FOUCHER, G. & BAFORT, J. M. (1977). Etude ultrastructurale des mitoses multiples au cours de la sporogonie du *Plasmodium b.berghei*. *Journal of Ultrastructural Research* **59**, 332–350.

SHAW, M. K. & TILNEY, L. G. (1992). How individual cells develop from a syncytium: merogony in *Theileria parva* (Apicomplexa). *Journal of Cell Science* **101**, 109–123.

SHAW, M. K., ROOS, D. & TILNEY, L. G. (1998). Acidic compartments and rhoptry formation in *Toxoplasma gondii*. *Parasitology* **117**, 435–443.

STEWART, M. J., SCHULMAN, S. & VANDERBERG, J. P. (1986). Rhoptry secretion of membranous whorls by *Plasmodium falciparum* merozoites. *American Journal of Tropical Medicine and Hygiene* **35**, 37–44.

TILNEY, L. G. & TILNEY, M. S. (1996). The cytoskeleton of protozoan parasites. *Current Opinion in Cell Biology* **8**, 43–48.

VAN WYE, J., GHORI, N., WEBSTER, P., MITSCHLER, R. R., ELMENDORF, H. G. & HALDAR, K. (1996). Identification and localization of rab6, separation of rab6 from ERD2 and implications for an 'unstacked' Golgi, in *Plasmodium falciparum*. *Molecular and Biochemical Parasitology* **83**, 107–120.

VICKERMAN, K. & COX, F. E. G. (1967). Merozoite formation in the erythrocytic stages of the malaria parasite *Plasmodium vinckei*. *Transactions of the Royal Society for Tropical Medicine and Hygiene* **61**, 303–312.

VIVIER, E. & PETITPREZ, A. (1972). Donées ultrastructurales complémentaires, morphologiques et cytochimiques, sur *Toxoplasma gondii*. *Protistologica* **8**, 199–221.

WARD, G. E., CHITNIS, C. E. & MILLER, L. H. (1994). The invasion of erythrocytes by malarial merozoites. In *Bailliére's Clinical Infectious Diseases*, *Vol 1* (*2*) *Strategies for Intracellular Survival* (ed. Russell, D. G.), pp. 155–190. Baillière Tindall, London.

WARD, G E., TILNEY, L. G. & LANGSLEY, G. (1997). GTPases and the unusual secretory pathway of *Plasmodium*. *Parasitology Today* **13**, 57–62.

WEBB, S. E., FOWLER, R. E., O'SHAUGHNESSY, C., PINDER, J. C., DLUZEWSKI, A. R., GRATZER, W. B., BANNISTER, L. H. & MITCHELL, G. H. (1996). Contractile protein system in the asexual stages of the malaria parasite *Plasmodium falciparum*. *Parasitology* **112**, 451–457.